Int. J. Electrochem. Sci., 7 **(2012)** 1214 - 1229

International Journal of
ELECTROCHEMICAL
SCIENCE
www.electrochemsci.org

Synthesis and Characterization of a Soluble Electrochromic Material: Poly(1,4-Bis(2-Thienyl)-Naphthalene) with Good Green Fluorescence Property

Chuan Li[1], *Min Wang*[1,2], *Chuansheng Cui*[1,*], *Lianyi Xu*[1], *Zhong Wang*[2], *Tianyu Kong*[3]

[1] Shandong Key Laboratory of Chemical Energy-storage and Novel Cell Technology, Liaocheng University, 252059, Liaocheng, P. R. China.
[2] The Central Laboratory of Liaocheng Hospital, 252000, Liaocheng, P. R. China
[3] State key Laboratory of Electronic Thin Films and Integrated Devices(UESTC)
[*]E-mail: cuichuansheng@163.com

Received: 12 December 2011 / *Accepted:* 17 January 2012 / *Published:* 1 February 2012

1,4-Bis(2-thienyl)-naphthalene (BTN) monomer is successfully synthesized via coupling reaction. Direct anodic oxidation of BTN monomer leads to the formation of a novel poly(1,4-bis(2-thienyl)-naphthalene) (PBTN) on a platinum wire in acetonitrile (ACN). The resultant polymer is investigated by cyclic voltammetry (CV) and characterized by FT-IR, ^{1}H NMR, and UV–vis spectra. The oligomer of resultant polymer is soluble in N, N-dimethyl formamide (DMF) and dimethyl sulfoxide (DMSO). Fluorescence spectra studies reveal that PBNT is a green-light emitter (emission at 514 nm) and the photoluminescence (PL) quantum yield (Ø) is 0.235 in DMF solution. According to the spectroelectrochemical analyses, PBTN film presents multielectrochromic property and shows four different colors under various potentials. Electrochromic switching of PBTN film is performed and the polymer film shows a maximum optical contrast (ΔT %) of 24% at 700 nm in visible region with a response time of 1.78 s. The coloration efficiency (CE) of PBTN is calculated to be 124.8 cm^2 C^{-1}. The multichromic polymer is thermally stable up to 496 ºC. SEM images illustrate that the polymer film presents a porous structure.

Keywords: Electrochemical polymerization, Conjugated polymer, Fluorescence, Electrochromism, Poly(1,4-bis(2-thienyl)-naphthalene).

1. INTRODUCTION

π-Conjugated polymers have been considered as promising materials holding unique optical and electrical properties [1], and have been widely applied in the fields of polymer solar cells (PSCs) [2], electrochromic devices [3, 4], sensors [5], polymer light emitting diodes (PLEDs) [6], and so on.

These electroactive and photoactive polymers are usually based on thiophene, pyrrole, phenylene, fluorene, or carbazole moieties. Recently, electrochromic (EC) polymers have drawn a lot of attentions due to their outstanding coloration efficiency [7], fast switching times [8], multiple colorations with the same material [3], fine-tunability of the band gap (and the color) [9], high stability [10], thin film flexibility and cost effectiveness [11]. For EC polymers, the electrochromism is related to the changing of band gaps during the doping-dedoping process [12, 13]. Thus, in order to achieve different properties EC polymers, an effective way is to adjust the electronic character of the π-orbit along the neutral polymer backbone, including main chain and pendant group structural modification and copolymerization [13-15].

Among electrochromic materials, thiophenes are a class of important EC conjugated polymers because of their high electrical conductivity and good redox property. They exhibit fast response time, outstanding stability and high contrast ratios in the visible and NIR regions in their electrochromic applications [8]. Moreover, they have facile E_g tunability through structural modifications, which have been reported extensively in past few years [16, 17]. Many polybithiophenes with alternating aromatic units have been synthesized and characterized, and it have been shown that the modification in the localization and aromaticity of the main polymer conjugation chain considerably influence the optical and electrochromic properties of the polythiophenes. More recently, it has been shown that the introduction of naphthalene bridge in the bithiophene polymer main chains could result in changed HOMO-LUMO band gap polymers compared with both homopolymers [27]. Furthermore, the broad range of substitution possibilities on naphthalene rings or on thiophene rings render possibilities to obtain tunable band gap electrochromic materials [28]. However, to the best of our knowledge, there are still no reports on the electrochromic and fluorescent properties of poly(1,4-bis(2-thienyl)-naphthalene) (PBTN).

In this study, 1,4-bis(2-thienyl)-naphthalene (BTN) monomer was synthesized via coupling reaction according to Scheme 1 [27]. In BTN monomer structure, the para position substitutions (thiophene) of the phenylene ring modify the degree of conjugation (extended π–π* bonding system) [29]. Due to the conjugated structures of the corresponding monomer, poly(1,4-bis(2-thienyl)-naphthalene) (PBTN) can be easily achieved by electrochemical polymerization of BTN monomer in 0.2 M $NaClO_4$/ACN solution with a much lower onset oxidation potentials (1.09V vs Ag-wire) than that of thiophene and naphthalene monomers [20, 30]. It is worth noting that the resultant polymer is partly soluble in N,N-dimethyl formamide (DMF) and possesses good green fluorescence property (emission at 514 nm).

The resultant polymer film also presents unique multicolor electrochromic properties (yellowish green color at neutral state, green color at intermediate doped state and blue color at full doped state) due to the introduction of naphthalene units into poly(2,2-bithiophene) backbone. It is interesting that many different tones of green color could be observed on the ITO glass surface by the partly oxidation of the neutral film.

The obtained PBTN polymer is characterized via cyclic voltammetry, SEM, UV–vis and FT-IR spectra. The spectroelectrochemical and electrochromic properties of the PBTN are also investigated in details.

2. EXPERIMENTAL

2.1. Materials

1,4-Dibromonaphthalene, and 2-bromothiophene are purchased from Aldrich Chemical and are used as received. Commercial high-performance liquid chromatography grade acetonitrile (ACN, Tedia Company, INC. USA) are used directly without further purification. Sodium perchlorate ($NaClO_4$, Shanghai Chemical Reagent Company, 98%) is dried in vacuum at 60 ºC for 24h before use. Other reagents are all used as received without further treatment.

2.2. Synthesis of 1,4-bis(2-thienyl)-naphthalene

The 1,4-bis(2-thienyl)-naphthalene (BTN) monomer was synthesized according to the Scheme 1. 2-Bromothiophene is reacted with magnesium to afford Grignard reagents which are then cross-coupled to 1,4-dibromonaphthalene in the presence of catalytic bis(triphenylphosphino) dichloronickel (II) ($NiCl_2(PPh_3)_2$). The purified product is a light-green white crystal. ^{1}H NMR and FT-IR verified the structure and purity of the BTN monomer.

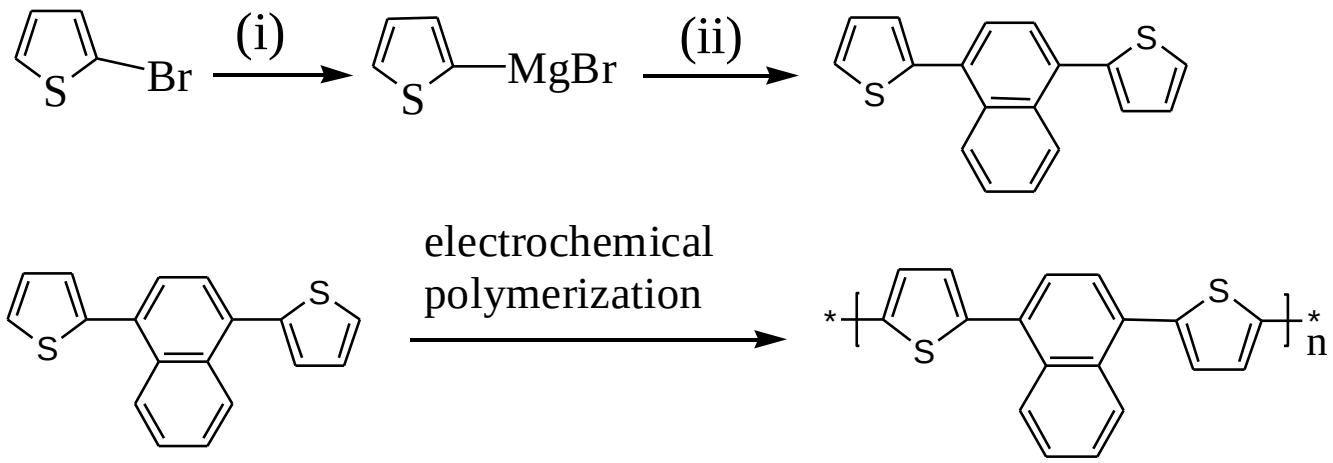

Scheme 1. Synthetic routes of monomer and polymer. Reagents: (i) Mg, Et_2O; (ii) 1,4-dibromonaphthalene, $NiCl_2(PPh_3)_2$, THF.

2.3. Characterizations

^{1}H NMR spectroscopy studies are carried out on a Varian AMX 400 spectrometer, and tetramethylsilane (TMS) is used as the internal standard for ^{1}H NMR. FT-IR spectra are recorded on a Nicololet 5700 FT-IR spectrometer, where the samples are dispersed in KBr pellets. UV–vis spectra are measured with a Perkin-Elmer Lambda 900 UV–vis–near-infrared spectrophotometer. Thermal behavior of the polymers is investigated via a Netzsch STA449C TG/DSC simultaneous thermal analyzer under nitrogen (N_2) atmosphere in the temperature range of 30 ~ 800 ºC with a heating rate of 10 ºC min^{-1}. With an F-4500 fluorescence spectrophotometer (Hitachi), fluorescence spectra are

determined. Scanning electron microscopy (SEM) measurements are taken by using a Hitachi SU-70 thermionic field emission SEM. The photographs of electrochromic films and fluorescence are taken by a Fujifilm Shot (FinePix F200EXR) digital camera. The fluorescence quantum yield (Ø) of dedoped PBTN dissolved in DMF is measured using anthracene in acetonitrile ($Ø_{ref}$ = 0.27) as the reference [31, 32] and is calculated according to the well-known method given as Eq.(1):

$$\phi = \frac{n^2 A_{ref} I}{n_{ref}^2 A I_{ref}} \phi_{ref} \qquad (1)$$

Here, *n* is the refractive index of the solvent, *A* is the absorbance at the excitation wavelength, and *I* is the intensity of the emission spectrum. The subscript *ref* denotes the reference, and no subscript denotes the sample. Absorbance of the samples and the standard should be similar [33].

2.4. Electrochemistry

Electrochemical syntheses and experiments is carried out in a one-compartment cell with a CHI 760 C Electrochemical Analyzer under computer control, employing a platinum wire with a diameter of 0.5 mm as working electrode, a platinum ring as counter electrode, and a silver wire (Ag wire) as pseudo reference electrode.

The working and counter electrodes for cyclic voltammetric experiments are placed 0.5 cm apart during the experiments. The electrolytes used are 0.2 M $NaClO_4$ in ACN solution. The electrodeposition is performed from a 0.005 M solution of the monomer in the electrolyte potentiodynamically at a scan rate of 100 mV s^{-1} or potentiostatically at 1.30 V vs. Ag wire. The pseudo reference is calibrated externally using a 5 mM solution of ferrocene (Fc/Fc^+) in the electrolyte ($E_{1/2}(Fc/Fc^+)$ = + 0.20 V vs. Ag wire in 0.2 M $NaClO_4$/ACN) [8]. Cyclic voltammetry of polymer is carried out using the same electrode set-up in monomer-free electrolyte solution.

All of the electrochemistry experiments are carried out at room temperature under nitrogen atmosphere.

2.5. Spectroelectrochemistry

Spectroelectrochemical data are recorded on Perkin-Elmer Lambda 900 UV-vis-near-infrared spectrophotometer connected to a computer. A three-electrode cell assembly is used where the working electrode is an ITO-coated glass slides (sheet resistance: < 10 Ω $□^{-1}$, purchased from Shenzhen CSG Display Technologies (China)), the counter electrode is a stainless steel wire, and an Ag wire is used as pseudo reference electrode. The potentials are reported versus Ag wire. Polymer films for spectroelectrochemistry are prepared by potentiostatically deposition on ITO glass slides (the active area : 2.1×0.8 cm^2).

3. RESULTS AND DISCUSSION

3.1. ^{1}H NMR spectrum, FTIR spectrum of BTN monomer

^{1}H NMR spectrum of BTN (Fig. 3A): $C_{18}H_{12}S_2$, δ_H (pm, DMSO-d_6) 8.236 (dd, 2H), 7.740 (d, 2H), 7.612 (4H), 7.360 (d, 2H), 7.275 (t, 2H). The assignments of the ^{1}H NMR lines are shown in the inset of the spectrum. The protons of naphthalene ring are observed at 8.236, 7.612 pm. Note that the ^{1}H NMR lines of the proton at *b* positions are overlapped with that of the proton at *c* positions, which have equivalent chemical shift at 7.612 pm. The protons of thiophene ring are at 7.740 (α-proton), 7.360 (β-proton) and 7.275 pm (β-proton), respectively.

FT-IR spectrum of BTN is shown in Fig. 4a. In the spectrum of BTN, the band around 1581 cm^{-1} is ascribed to the stretching vibrations of phenylene rings, and the bands at 1506 and 1457 cm^{-1} are due to the stretching vibrations of thiophene rings [34, 35]. A strong absorption located at 697 cm^{-1} is assigned to the out-of-plane bending vibrations of C–H bonding in the monosubstitued thiophene rings. The 764 cm^{-1} band is assigned to the out-of-plane vibration of the 4 adjacent C–H bonds in the substituted phenylene rings and that of the two adjacent C–H bonds is at 873, 846 and 815 cm^{-1} [20, 36], indicating the presence of 1,4-disubstitued naphthalene unit in the monomer.

3.2. Electrochemical polymerization and characterization of PBTN

3.2.1 Electrochemical polymerization of PBTN

The successive CV curves of 0.005 M BTN in 0.2 M $NaClO_4$/ACN are illustrated in Fig. 1. As the CV scan continued, PBTN film is formed on the working electrode surface. The increases in the redox wave current densities imply that the amount of conducting polymers deposited on the electrode are increasing [37].

The CV curves of BTN show distinct reduction waves of the oligomer located at 0.86 V, while the corresponding oxidation waves are overlapped with the oxidation waves of the BTN monomer and cannot be observed clearly [38].

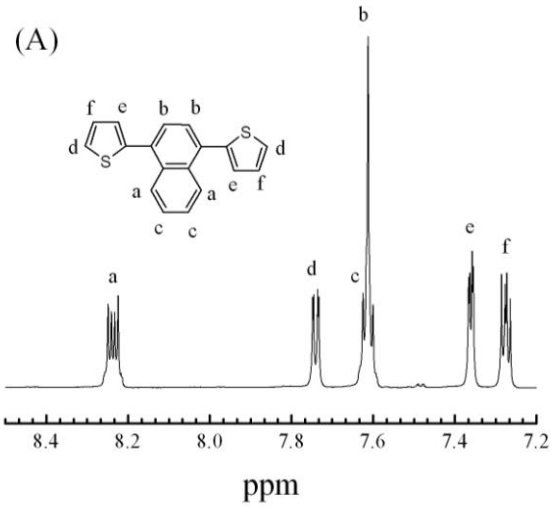

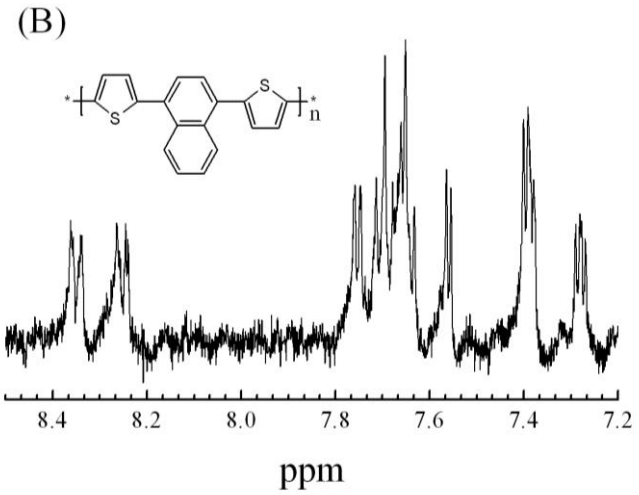

Figure 1. (A) ^{1}H NMR spectrum of 1,4-bis(2-thienyl)-benzene monomer in DMSO-d_6. Insert: the structure of the monomer. (B) ^{1}H NMR spectrum of poly(1,4-bis(2-thienyl)-benzene) in DMSO-d_6. Inset: the structure of the polymer.

3.2.2. Electrochemistry behavior of the polymer films

Fig.2 shows the electrochemical behavior of the PBTN film (prepared on platinum wires by sweeping the potentials from 0 and 1.3 V for ten cycles) at different scan rates between 50 and 300 mV s^{-1} in 0.2 M $NaClO_4$/ACN. As can be seen from Fig. 2a, the PBTN film is cycled repeatedly between doped and dedoped states without significant decomposition. The peak current densities (j) are proportional to the potential scan rates (Fig. 2b), indicating a reversible redox process of the polymer adhering to the platinum wire electrode [38]. This also demonstrates that the electrochemical processes of the polymer are reversible and not diffusion limited [36, 39].

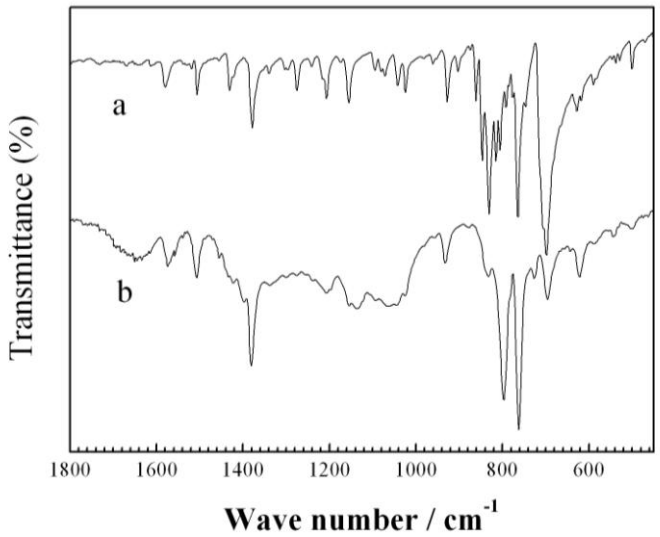

Figure 2. The FT-IR spectra of (a) 1,4-bis(2-thienyl)-benzene monomer and (b) PBTN prepared at 1.30 V potentiostatically.

3.2.3. ^{1}H NMR and FTIR spectra of PBTN

The ^{1}H NMR spectrum of PBTN prepared at 1.3 V potentiostatically is recorded in DMSO-d_6, as shown in Fig. 3B. The spectrum of PBTN shows eight groups of protons between 7.2 and 8.4 pm, which are located within the low field compared with that of BTN due to the high conjugation length of the polymer chain [40]. Compared with the ^{1}H NMR spectrum of BTN monomer, the disappearance of the ^{1}H NMR lines of the proton at *d* positions in the the spectrum of PBTN indicated that the ring coupling reaction during the electrochemical polymerization process eliminated the protons at the *d* positions of the monomer [41]. Thus, the structure of the polymer can be reasonably postulated as shown in the inset of Fig. 3B.

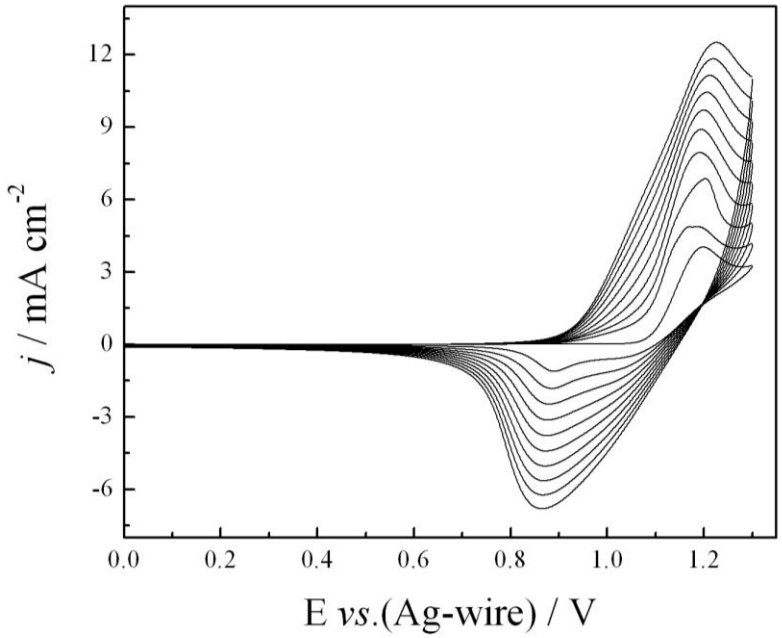

Figure 3. Cyclic voltammogram curves of 0.005 M BTN in 0.2 M $NaClO_4$/ACN solutions at a scan rate of 100 mV s^{-1}.

To obtain a sufficient amount of PBTN for characterization, the ITO glass with a surface area of 1.6 cm^2 is employed as working electrodes. The polymer is synthesized at 1.3 V vs. Ag wire potentiostatically in the solution of 0.2 M $NaClO_4$/ACN containing 0.005 M monomer. Fig. 4b shows the FT-IR spectrum of PBTN. The absorption bands at 796 and 1059 cm^{-1} are attributed to the out-of-plane and in-plane bending vibrations of C–H bonding in β-position of the 2,5-disubstitued thiophene rings, respectively [42]. Compared with the spectrum of BTN, the occurrence of a new strong absorptions located at 796 cm^{-1} and the diminution of the strong peak at 697 cm^{-1} in the spectrum of PBTN imply that the polymerization of the BTN monomer occurs at the α-position of thiophene rings (see Scheme 1).

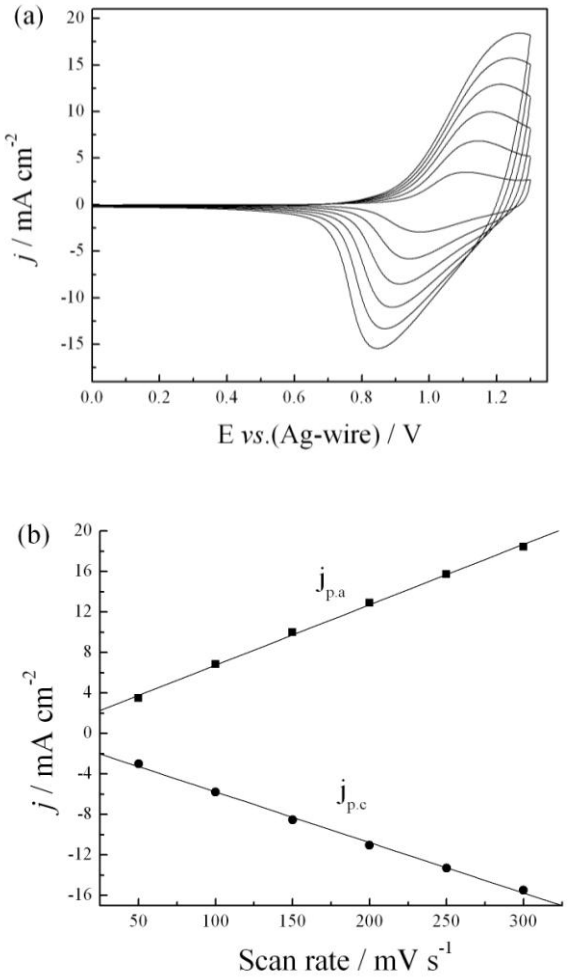

Figure 4. (a) CV curves of the PBTN film at different scan rates between 30 mV s^{-1} and 300 mV s^{-1} in the monomer-free 0.2 M $NaClO_4$/ACN. (b) scan rate dependence of the PBTN. j_{pa} and j_{pc} denote the anodic and cathodic peak current densities, respectively.

3.2.4 Optical Properties

The oligomer of PBTN is soluble in N,N-dimethyl formamide (DMF) and dimethyl sulfoxide (DMSO). The UV-visible spectrum of PBTN dissolved in DMF solution shows a strong and sharp absorption peak at 384 nm (Fig. 5a) and the energy gap is calculated as 2.59 eV. The UV–vis spectrum of the dedoped PBTN film electrodeposited on ITO electrode at 1.30 V potentiostaticall is shown a broad π–π* absorption maxima around 401 nm (Fig. 5b) and the energy gap is 2.33 eV. It is worth noting that there is a slight red shift of the absorption maxima of the dedoped PBTN film deposited on ITO electrode compared with that of the corresponding polymer dissolved in DMF. The reasonable explanation for this phenomenon might be that among the solid state polymer, there are some polymer molecules with greater polymerization degrees, which are insoluble in DMF. As a result, the average conjugation degree of solid state polymer is higher than that of the corresponding polymer dissolved in DMF, which lead to the red shift of the solid state polymer[37]. Meanwhile, the UV–visible spectrum of BTN monomer in DMF solution is also investigated. As can be seen from Fig. 5c (see inset), the

absorption maximum of BTN monomer are centered at 327 nm. The difference between the λ_{max} values of the monomer and PBTN dissolved in DMF is about 57 nm, which is owing to the increased conjugation length in the polymer compared with the monomer [20].

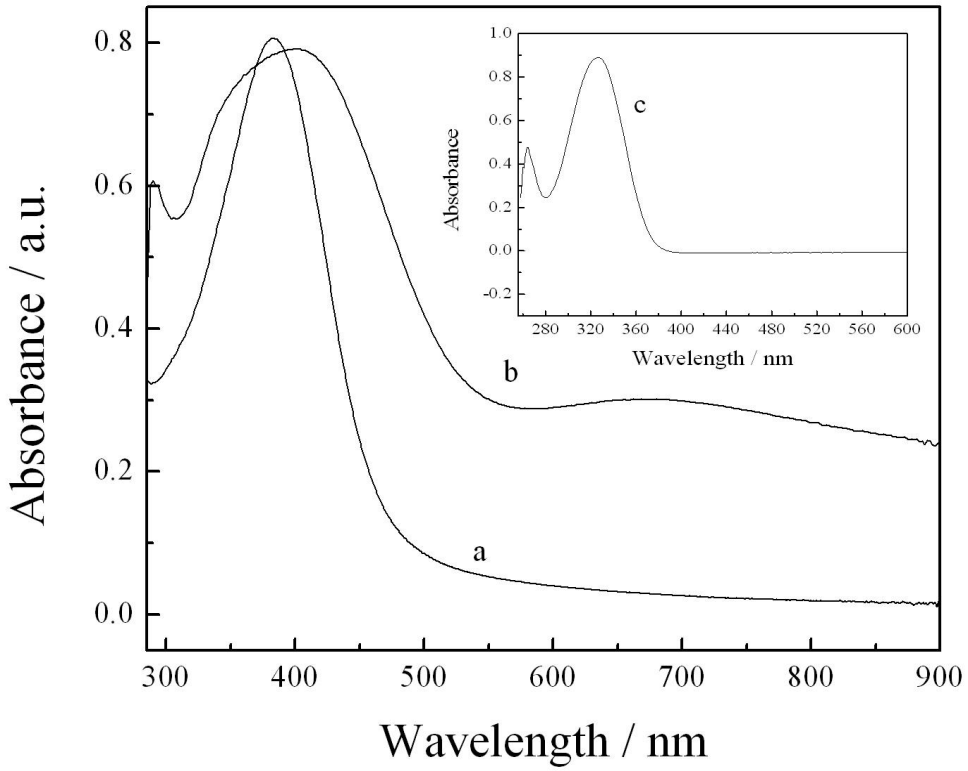

Figure 5. UV–vis spectra of (a) PBTN dissolved in DMF, (b) PBTN deposited on ITO electrode. Inset: UV–vis spectrum of (c) BTN monomer dissolved in DMF.

3.2.5. Fluorescence property

The fluorescence properties of PBTN dissolved in DMF are also measured. As shown in Fig. 6, PBTN exhibits a maximum excitation peak at 391.5 nm in visible region (Fig. 6a), and a strong emission peak of PBTN is at 514.5 nm in the green region (Fig. 6A). Compared with the fluorescence properties of poly(1,4-bis(2-(3-octyl)thienyl)-naphthalene) (blue-green light emission with a 31% fluorescence quantum yield) [28], PBTN presents a valuable green fluorescence property. For the BTN monomer, its emission peak is located at 428.5 nm in the blue region (Fig. 6B). The red shift of the emission peak compared with that of monomer further proved the formation of conjugated backbone of PBTN, in well agreement with the UV–vis spectral results (see Fig. 5). The fluorescence quantum yield (Ø) of as-formed PBTN in DMF is measured to be 0.235 according to the Eq. (1). These fluorescent results imply that the soluble PBTN may be a good candidate in green-light-emitting materials, which could be exploited for many applications, such as organic lasers.

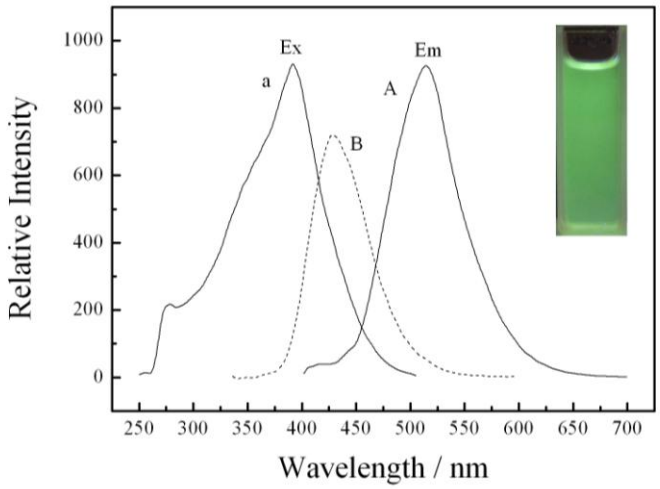

Figure 6. Fluorescence spectra of PBTN and BTN monomer dissolved in DMF. Emission spectra of (A) PBTN, (B) BTN monomer. Excitation spectrum of (a) PBTN. Inset: Photoluminescence of PBTN dissolved in DMF under UV light irradiation of 365 nm.

3.2.6. Scanning electron microscopy of PBTN film

The properties of conducting polymers are strongly dependent on their morphology and structure [40]. The polymer film of PBTN is prepared potentiostatically at 1.3 V vs. Ag wire from the solution of 0.2 M $NaClO_4$/ACN containing 0.005 M monomer on ITO electrodes. The surface morphology of the neutral PBTN is investigated by scanning electron microscopy (SEM) after depoding at –0.1V for 10 min in 0.2 M $NaClO_4$/ACN. The PBTN film exhibits a porous structure like coral grown with small granules (Fig.7), and the approximate diameters of these globules are in the range of 50 ~ 200 nm. This morphology of PBTN may facilitate the movement of doping anions into and out of the polymer film during doping and dedoping process, being in agreement with the good redox activity of PBTN.

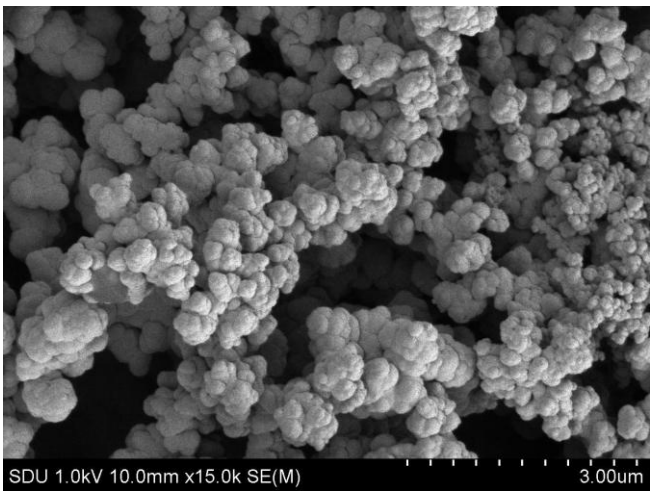

Figure 7. SEM image of PBTN deposited on ITO electrode at 1.30 V potentiostatically.

3.2.7. Thermal analysis

The thermal stability of a conjugated polymer is very important for its potential application [43, 44]. The thermal stability of PBTN in dedoped state is analyzed under nitrogen atmosphere in the temperature range of 30 ~ 800 ºC with a heating rate of 10 ºC min^{-1}. The thermogravimetry (TG) curve of the polymer is shown in Fig. 8a. According to Fig. 8a, before 149 ºC, a light weight loss of PBTN is about 3.5 %, mainly due to evaporation of water trapped in the polymers [40]. After 496 ºC, the further increase in temperature results in the significant weight loss for polymer with the weight loss rate at 2.88 % min^{-1}, which is due to the degradation of the backbone of PBTN. All the results indicate that the polymer presents a good thermal stability.

The differential scanning calorimetry (DSC) measurements of the PBTN is also performed at the same time. According to the differential scanning calorimetry (DSC) curve of PBTN (Fig. 8b), the polymer presents one sharp exothermic peak at 545 ºC and one strong endothermic peak at 720 ºC. The results indicate that there is a thermal decomposition reaction at the region of the temperature, in well agreement with the TG result.

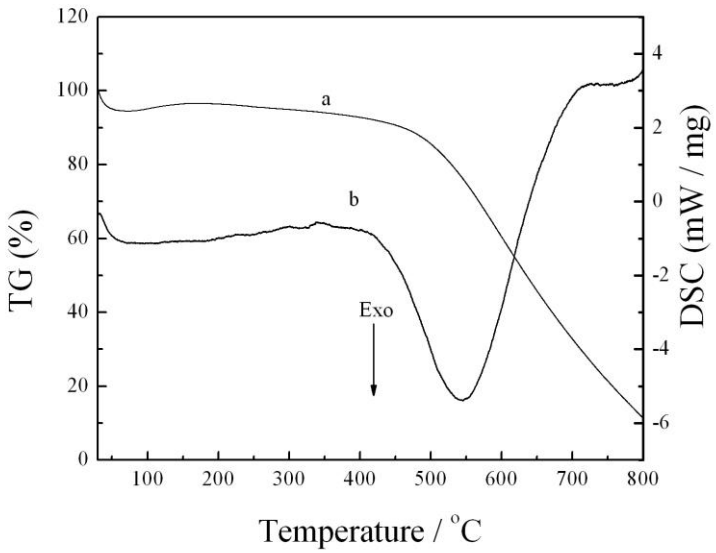

Figure 8. (a) TG curve and (b) DSC curve of PBTN under nitrogen atmosphere in the temperature range of 30~800 ºC with a heating rate of 10 ºC min^{-1}.

3.3. Electrochromic properties of PBTN

3.3.1. Spectroelectrochemical properties of PBTN

Spectroelectrochemistry is used to obtain information about the electronic structure of PBTN and to examine the spectral changes which occur during redox switching. PBTN coated ITO (prepared potentiostatically at 1.3 V vs. Ag wire) is switched between 0 and 1.3 V in 0.2 M $NaClO_4$/ACN system in order to obtain the in situ UV-vis spectra (Fig. 9). As shown in Fig. 9, the intensity of the PBTN π–π* electron transition absorption decreases while two charge carriers absorption bands located at 700

nm and longer than 1050 nm increase dramatically upon oxidation. Furthermore, it is interesting to find that the PBTN film shows a multicolor electrochromism. During the oxidation process, yellowish green color of the film at neutral state (0 V) turns into green color at intermediate doped state (1.1 V), and then into blue color at full doped state (1.3 V). The colors of the electrochromic materials are defined accurately by performing colorimetry measurements. CIE system is used as a quantitative scale to define and compare colors. Three attributes of color: hue (a), saturation (b) and luminance (L) are measured and recorded. These colors and corresponding L, a, b values are given in Fig. 10.

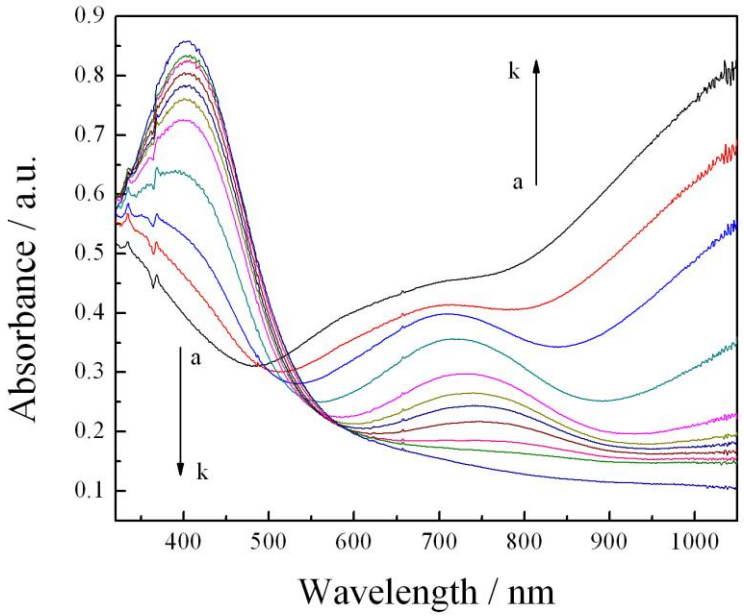

Figure 9. Spectroelectrochemical spectra of PBTN with applied potentials between 0 V and +1.3 V in 0.2 M $NaClO_4$ / ACN. Applied potentials are the following: (a) 0 V; (b) 0.7 V; (c) 0.8 V; (d) 0.9 V; (e) 0.95 V; (f) 1.0 V; (g) 1.05 V; (h) 1.1 V; (i) 1.15 V; (j) 1.2 V; (k) 1.3 V.

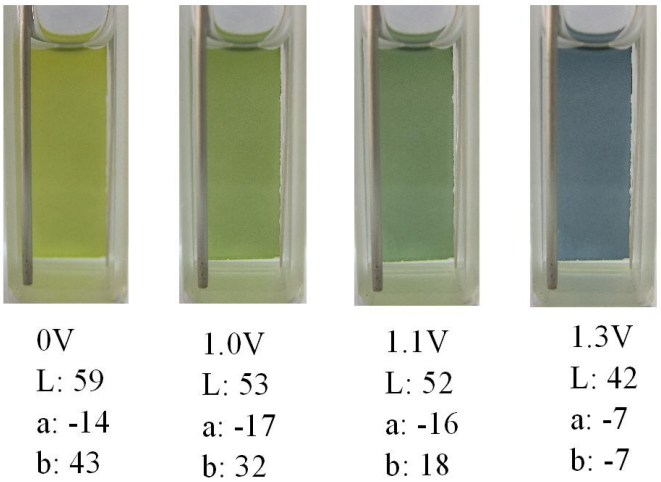

Figure 10. The images of PBTN film at 0 V (the neutral state), 1.0V (the intermediate doped state), 1.10V (the intermediate doped state) and 1.30 V (the full doped state).

3.3.2. Electrochromic switching of PBTN film in solution

It is important that polymers can switch rapidly and exhibit obvious color changes, revealing superior results in electrochromic applications [45]. The dynamic electrochromic experiment for PBTN is carried out at 700 nm, where the maximum transmittance differences between redox states are observed in the visible region. Square wave potential step method is coupled with optical spectroscopy, named chronoabsorptometry, to investigate the switching ability of PBTN between its neutral and doped state (Fig. 11). The potential is interchanged between 0 (the neutral state) and 1.3 V (the oxidized state) with a residence time of 4 s. One important characteristic is the optical contrast (ΔT %), which can be defined as the transmittance difference between the redox states. The ΔT % of the PBTB is found to be 24 % at 700 nm, as showed in Fig. 11.

The coloration efficiency (CE) is also an important characteristic for the electrochromic materials. CE can be calculated by using the equations and given below [46]:

$$\Delta \mathrm{OD} = \lg\left(\frac{T_\mathrm{b}}{T_\mathrm{c}}\right) \quad \text{and} \quad \eta = \frac{\Delta \mathrm{OD}}{\Delta \mathrm{Q}}$$

where T_b and T_c are the transmittances before and after coloration, respectively. ΔOD is the change of the optical density, which is proportional to the amount of created color centers. η denotes the coloration efficiency (CE). ΔQ is the amount of injected charge per unit sample area. CE of PBTB film is measured as 124.8 cm^2 C^{-1} (at 700 nm) at full doped state, which had reasonable coloration efficiency.

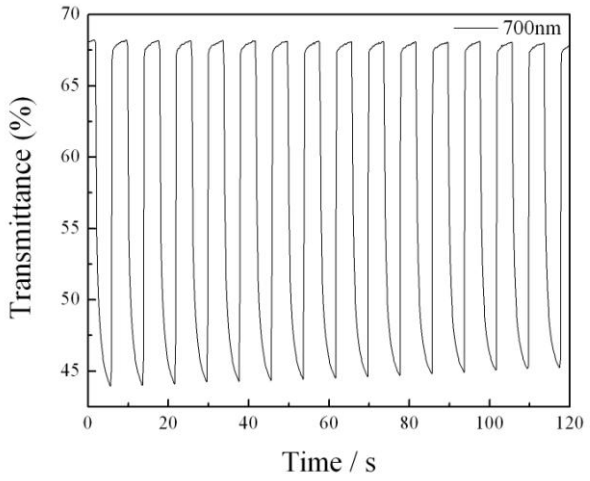

Figure 11. Electrochromic switching (700 nm) for PBTN film monitored in 0.2 M $NaClO_4$/ACN solution under an applied square voltage signal between 0 V and +1.30 V with a residence time of 4 s.

Response time, one of the most important characteristics of electrochromic materials, is the time needed to perform a switching between the neutral state and oxidized state of the materials [39,

45]. The response required to attain 95% of total transmittance difference is found to be 1.78 s from the reduced to the oxidized state and 0.36 s from the oxidized to the reduced state. Thus, PBTN can be rapidly switched to the reduced state, which can be attributed to the ease of charge transport in the conducting film when it is reduced [47].

3.3.3. Stability of PBTN film

The stability of EC materials toward long-term switching between the neutral and oxidized states is one of the most important factors for the application of EC materials in device utilities. For this reason, the as-prepared PBTN film on ITO electrode is tested by cycling of the applied potential between –0.1 and +1.4 V with 500 mV/s in propylene carbonate (PC) solution containing 0.2 M lithium perchlorate ($LiClO_4$) to evaluate the stability of the film (Fig. 12). After 500 cycles, 84.5% of its original electroactivity is retained and the changes in anodic (j_{pa}) and cathodic peak current densities (j_{pc}) are 16% and 28%, respectively.

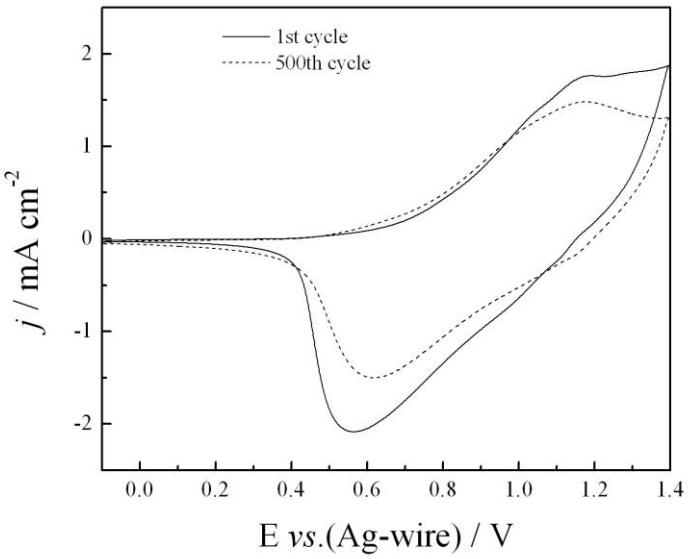

Figure 12. Cyclic voltammogram of PBTN film in 0.2 M $LiClO_4$/PC by cycling of the applied potential between –0.1 and +1.4 V with 500 mV/s.

4. CONCLUSION

1,4-Dis(2-thienyl)-naphthalene monomer containing naphthalene and thiophene units is synthesized by coupling reaction. And then, its polymer is successfully synthesized by electrochemical oxidation of the monomer in 0.2 M $NaClO_4$/ACN solution. The obtained polymer film is characterized by cyclic voltammetry (CV), TG, UV–vis, FT-IR and ^{1}H NMR spectra. It is interesting that poly(1,4-bis(2-thienyl)-naphthalene) (PBTN) is partly solubly in DMF and DMSO and possesses good redox activity and thermal stability. The fluorescence spectra studies indicate that the soluble polymer is a

green-light emitter and the photoluminescence (PL) quantum yield (Ø) is 0.235 in DMF solution. PBTN film deposited on ITO glass presents multicolor electrochromic properties (yellowish green color at neutral state, green color at intermedia doped state and blue color at full doped state). Electrochromic switching of PBTN film is performed and the polymer film shows a maximum optical contrast (ΔT %) of 24% at 700 nm in visible region with a response time of 1.78 s. The coloration efficiency (CE) of PBTN is calculated to be 124.8 cm^2 C^{-1}. The new multichromic polymer is thermally stable up to 496 ºC. These properties make PBTN a good candidate for commercial applications.

ACKNOWLEDGEMENTS

The work was financially support by the National Natural Science Foundation of China (20906043), the Promotive research fund for young and middle-aged scientists of Shandong Province (2009BSB01453), the Natural Science Foundation of Shandong province (ZR2010BQ009), the open foundation of the State key Laboratory of Electronic Thin Films and Integrated Devices(KFJJ201114) and the Taishan Scholarship of Shandong Province.

References

1. M. Hanif, P. Lu, M. Li, Y. Zheng, Z.Q. Xie, Y.G. Ma, D. Li, J.G. Li, *Polym. Int*., 56 (2007) 1507.
2. J. Y. Kim, K. Lee, N. E. Coates, D. Moses, T. Q. Nguyen, M. Dante, A. J. Heeger, *Science*, 317 (2007) 222.
3. A.Yildirim, S. Tarkuc, M. Ak, L. Toppare, *Electrochim. Acta*, 53 (2008) 4875.
4. M. Ak, E. Sahmetlioglu, L. Toppare, *J. Electroanal.Chem*., 621 (2008) 55.
5. J. Chen, C. Too, G. Wallace, A. Burrell, G. Collis, D. Officer, G. Sweigers, *Electrochim. Acta*, 47 (2002) 2715.
6. R. H. Friend, R. W. Gymer, A. B. Holmes, J. H. Burroughes, R. N. Marks, C. Taliani, D. D. C. Bradley, D. A. Dos Santos, J. L. Brédas, M. Lögdlund, W. R. Salaneck, *Nature*, 397 (1999) 121.
7. G. Sonmez, H. Meng, F. Wudl, *Chem. Mater*. 16 (2004) 574.
8. G. Sonmez, C. K. F. Shen, Y. Rubin, F. Wudl, *Angew. Chem. Int. Ed*. 43 (2004) 1498.
9. E. Yildiz, P. Camurlu, C. Tanyeli, I. Akhmedov, L. Toppare, *J. Electroanal. Chem*. 612 (2008) 247.
10. M. Li, A. Patra, Y. Sheynin, M. Bendikov, *Adv. Mater*. 21 (2009) 1707.
11. C. Ma, M. Taya, C.Y. Xu, *Electrochim. Acta*, 54 (2008) 598.
12. F. B. Koyuncu, S. Koyuncu, E. Ozdemir, *Electrochim. Acta*, 55 (2010) 4935.
13. C. Zhang, C. Hua, G, H, Wang, M. Ouyang, C.A. Ma, *J. Electroanal. Chem*. 645 (2010) 50.
14. J. Seixas de Melo, J. Pina, H.D. Burrows, R.E. Di Paolo, A.L. Mac¸anita, *Chem. Phys*. 330 (2006) 449.
15. A.Bessiere, C. Duhamel, J.C. Badot, V. Lucas, M.C. Certiat, *Electrochim. Acta* 49 (2004) 2051.
16. C. Pozo-Gonzalo, M. Salsamendi, J.A. Pomposo, H.J. Grande, E.Y. Schmidt, Y.Y. Rusakov, B.A. Trofimov, *Macromolecules*, 41 (2008) 6886.
17. Y. Pang, X. Li, H. Ding, G. Shi, L. Jin, *Electrochim. Acta*, 52 (2007) 6172.
18. S. Tasch, W. Graupner, G. Leising, L. Pu, M.W. Wagner, R.H. Grubbs, *Adv. Mater*. 7 (1995) 903.
19. G. Zu, W.K. Luo, H.Q. Wu, *Acta Chim. Sin*. 57 (1999) 465.
20. Z.M. Huang , L.T. Qu, G.Q. Shi, F.E. Chen, X.Y. Hong, *J. Electroanal. Chem*. 556 (2003) 159.
21. G. Shi, G. Xue, C. Li, S. Jin, *Polym. Bull*. 33 (1994) 325.
22. S. Hara, N. Tashima, *Chem. Lett*. (1990) 269.

23. M. Rani, R. Ramachandran, S. Kabilan, *Synth. Met*., 160 (2010) 678.
24. M. Jonforsen, I. Ahmad, T. Johansson, J. Larsson, L.S. Roman, M. Svensson, O. Inganäs, M.R. Andersson, *Synth. Met*., 119 (2001) 185.
25. S. Koyuncub, B. Gultekina, C. Zafera, H. Bilgili, M. Cana, S. Demica, İ. Kayab, S. Icli, *Electrochim. Acta*, 54 (2009) 5694.
26. M. Dietrich, J. Heinze, G. Heywang, F. Jonas, *J. Electroanal. Chem*., 369 (1994) 87.
27. A.M. Fraind, J.D. Tovar, *J. Phys. Chem*. B 114 (2010) 3104.
28. W.-L. Wang, Y.-H. Lai, *Thin Solid Films* 471 (2002) 211.
29. S. Ayachi, K. Alimi, M. Bouachrine, M. Hamidi, J.Y.Mevellec, J.P. L'ere-Porte, *Synth. Met*. 156 (2006) 318.
30. A.Durmus, G.E. Gunbas, P. Camurlu, L. Toppare, *Chem. Commun*. 31 (2007) 3246.
31. C. Zimmermann, M. Mohr, H. Zipse, R. Eichberger, W. Schnabel, *J. Photochem. Photobiol. A Chem*., 125 (1999) 47.
32. B.Y. Lu, L.Q. Zeng, J.K. Xu, Z.G. Le, H.Y. Rao, *Eur. Polym. J*., 45 (2009) 2279.
33. F.C. Tasi, C.C. Chang, C.L. Liu, W.C. Chen, S.A. Jenekhe, *Macromolecules*, 38 (2005) 1958.
34. C. Zhang, C. Hua, G, H, Wang, M. Ouyang, C.A. Ma, *J. Electroanal. Chem*. 645 (2010) 50.
35. S.C. Ng, J.M. Xu, H.S.O. Chan, A. Fujii, K. Yoshino, *J. Mater. Chem*. 9 (1999) 381.
36. C. Zhang, Y. Xu, N. Wang, Y. Xu, W. Xiang, M. Ouyang, C. Ma, *Electrochim. Acta*, 55 (2009) 13.
37. R. Yue, J.K. Xu, B.Y. Lu, C.C. Liu, Y.Z. Li , Z.J Zhu, S. Chen, *J. Mater. Sci*., 44 (2009) 5909.
38. G.W. Lu, G.Q. Shi, *J. Electroanal. Chem*., 586 (2006) 154.
39. B. Yigitsoy, S. Varis, C. Tanyeli, I.M. Akhmedov, L. Toppare, *Electrochim. Acta*, 52 (2007) 6561.
40. G.M. Nie, L.Y. Qu, J.K. Xu, S.S. Zhang, *Electrochim. Acta*, 53 (2008) 8351.
41. Z.H. Huang, G.Q. Shi, L.T. Qu, X.Y. Hong, *J. Electroanal. Chem*. 544 (2003) 41.
42. K. Kham, S. Sadki, C. Chevrot, *Synth. Met*. 145 (2004) 135.
43. E. Lim, B.J. Jung, H.K. Shim, *Macromolecules*, 36 (2003) 4288.
44. W. Ma, C. Yang, X. Gong, K. Lee, A.J. Heeger, *Adv. Funct. Mater*., 15 (2005) 1617.
45. G.M. Nie, L.J. Zhou, Q.F. Guo, S.S Zhang, *Electrochem. Commun*. 12 (2010) 160.
46. C. Bechinger, M.S. Burdis, J.-G. Zhang, *Solid State Commun*. 101 (1997) 753.
47. G.A. Sotzing, J.R. Reynolds, *Chem. Mater*. 8 (1996) 882.